Test for low-dimensional determinism in electroencephalograms

Jaeseung Jeong, Moo Seong Kim, and Soo Yong Kim
Department of Physics, Korea Advanced Institute of Science and Technology, Taejon 305-701, Korea
(Received 9 February 1999)

We tested low-dimensional determinism in an electroencephalogram (EEG), based on the fact that smoothness (continuity) on an embedded phase space is enough to imply determinism within time series. A modified version of the method developed by Salvino and Cawley [Phys. Rev. Lett. **73**, 1091 (1994)] was used. In our method, we chose a box randomly and then estimated the mean directional element in the box containing the $d+1$ data points, where d is the embedding dimension. The global average for the mean local directional elements over the boxes, W, is a measure for smoothness. The nonlinear noise reduction method developed by Sauer [Physica D **58**, 193 (1992)] is then applied to the EEG. We also compared the results for the EEG with those for its surrogate data. We found that the W values for the noise-reduced EEG had stable values around 0.35, which means that the EEG is not a low-dimensional deterministic signal. However, this method may not be applicable to the time series generated from high-dimensional deterministic systems. We cannot exclude the possibility that the determinism in the EEG may be too high-dimensional to be detected with current methods. [S1063-651X(99)05207-1]

PACS number(s): 87.80.Tq, 87.19.Nn, 87.90.+y

I. INTRODUCTION

Electroencephalogram (EEG) is a complex and aperiodic time series, which is a sum over a very large number of neuronal dendritic potentials. It is an important problem to decide whether the EEG is filtered noise or a deterministic signal. If the EEG is deterministic, then we can extract a lot of information on brain dynamics from the EEG, and then study brain functions with dynamical models from the EEG.

Whether the EEG is generated by a deterministic chaotic process or a linear stochastic one is still controversial. Babloyantz and Salazar first reported that the EEG data from the human brain during the sleep cycle had chaotic attractors for sleep stages II and IV [1]. A lot of research with nonlinear methods revealed that the EEG had a finite noninteger correlation dimension and a positive Lyapunov exponent, which means that the EEG is generated by a deterministic chaotic neural process [2–4]. Haken and his colleagues analyzed the spatio-temporal patterns of the EEG in epileptic seizures. These showed that the global dynamics of the EEG might be described by a nonlinear evolution equation with order parameters and a few principal patterns, which are intimately related to the degrees of freedom within the system [5–7]. Furthermore, there is some evidence that the distinct states of brain activity can also have different chaotic dynamics quantified by nonlinear dynamical measures [8–11]. These measures, even though as measures of complexity they are still informal instead of being used as absolute measures, can be used as a fruitful tool in differentiating the physiological and/or pathological brain states [12–17].

However, there are a number of technical problems in the implementation of current nonlinear dynamic algorithms with regard to such variables as data size, sampling rate, and stationarity that preclude an unambiguous interpretation of data sets [18–21]. Osborne and Provenzale demonstrated that the signals from $(1/f)$-like linear stochastic systems, so-called colored noise, also resulted in a finite correlation dimension [22]. Rapp *et al.* showed that the filtered noise could mimic low-dimensional chaotic attractors as the EEG data did [23]. Thus many of the claims for deterministic chaos in EEG data must bear critical examination and reevaluation.

By using the surrogate data methods, Theiler *et al.* found that the EEG was not produced by low-dimensional chaos [24,25]. Pritchard *et al.* also applied surrogate-data testing to a normal resting human EEG and revealed that a normal resting human EEG was nonlinear, but did not represent low-dimensional chaos [26]. Similar results have been independently reported by Casdagli [27], Rombouts *et al.* [28], and Palus [29].

Recently more direct methods have been developed to detect determinism within a time series [28–38]. The Sugihara-May method is based on how well past trajectories can predict the future [30]. The Kaplan-Glass method is based on the parallelness of a certain vector field reconstructed from the time-series data [32,33]. The methods proposed by both Wayland *et al.* [34] and Salvino and others [35–37] also measure the continuity of a vector series on an embedded phase space. These direct methods can be useful in identifying deterministic chaos in natural signals with broadband power spectra. They are also capable of distinguishing between chaos and a random process very effectively.

There are only a few studies on the application of these direct methods to the EEG [39–41]. Blinowska and Malinowski applied the Sugihara-May method to the EEG, and reported that the benefits in prediction from this method were similar to that of a linear autoregressive method. Mees used the tesselation method to predict one step ahead for the EEG [40]. The prediction is rather poor in some places, but in other places it is very good. She draws a conclusion carefully from this casual prediction simulation that determinism in EEG might exist. Glass and his colleagues tested with the Kaplan-Glass method for deterministic dynamics in both a real EEG and a simulated EEG generated by a neural network model [41]. They found similar orientations of tangents to the trajectory in a given small region of phase space from the simulated EEGs, but not from the real EEGs. They,

therefore, concluded that the real EEG data did not have any determinism. However, these studies were all preliminary since they used only small embedding dimensions of about 3–5, and did not consider the effects of noise in the EEG data.

In the present paper, we tested the low-dimensional determinism in the EEG more rigorously by using a modified version of the method which was originally proposed by Salvino and Cawley [35–37]. It is based on the fact that smoothness (continuity) on an embedded phase space is enough to imply determinism within a time series. We applied a nonlinear noise-reduction method to the EEGs in order to remove noise effects, and then used the minimum embedding dimension for a reconstruction of the attractor from the EEG in the phase space. Finally, we compared the results from the EEG with those from the surrogate data of the EEG.

II. ALGORITHMS FOR DETECTING SMOOTHNESS

The main step in our test is to detect smoothness of the vector fields in the phase space reconstructed from the EEG data. If the time series are generated from deterministic systems that are governed by nonlinear ordinary differential equations, then nearby points on the phase space behave similarly under time evolution. These smoothness properties thus imply determinism.

Let an observed time series $v(t)$ be the output of a differentiable dynamical system f^t on an m-dimensional manifold M. With delay coordinates and a sufficiently large embedding dimension d, an embedding of M into a d-dimensional reconstructed manifold R^d then typically results. The delay vector time series $x(t)=(v(t),v(t+\Delta),\ldots,v(t+(d-1)\Delta))$, where Δ is the time delay, lives in the embedded image of M in R^d. Smoothness of the dynamical system is preserved in the embedded image.

We denote a time-one map, i.e., f^1, by F and consider the following general quantity:

$$\phi=\phi(x)=\Psi(x,F^b(x),\ldots F^{b(R-1)}(x)),\quad R>1, \tag{1}$$

where F^b denotes the bth iterate of F, and Ψ is a smooth function of its R vector arguments into R^d. $\phi(x)$ is a vector field in R^d. If we take $b=1$ here for simplicity, then a simple form for $\phi(x)$ is

$$\phi(x)=\sum_{r=0}^{R-1} c_r F^r(x),\quad R>1. \tag{2}$$

F may be an arbitrarily sampled flow, or a map; $F^0(x(t))=x(t)$, $F^1(x(t))=x(t)$, $F^1(x(t))=x(t+1)$, etc. The c_r are arbitrary, and we now take them to be constants, independent of x.

Directional fields (unit vectors) for $\phi(x)$ in dynamical systems are smooth, and depend on the choice of the c_r. To estimate the smoothness of the fields, we can partition the phase space by a uniform grid in the Salvino-Cawley method. We call the jth mesh cell of points, comprised of the $x_i, i=1,\ldots,n_j$, box j. Then we can compute the average of the directional elements, $\hat{x}=\phi(x)\|\phi(x)\|^{-1}$, over box j, where $\|\phi(x)\|$ is a norm of $\phi(x)$.

$$Y_j=n_j^{-1}\sum_{i=1}^{n_j}\hat{x}(x_i). \tag{3}$$

Y_j is 1 for smooth data, and it decreases to 0 for random data. A global average of mean local directional elements over the boxes is a measure for smoothness, that is, determinism, in the vector field.

$$W=N^{-1}\sum_j n_j\|Y_j\|^2 \tag{4}$$

is just a weighted mean square of Y_j. If the data are smooth and boxes are sufficiently small, W is 1. W is, however, often a lot less than 1 owing to the finite numerics for smooth data. W depends on embedding parameters such as time delays and embedding dimensions.

W also depends on the choice of vector field ϕ. The natural choice $\{c_r\}=\{-1,1\}$, implicit in the method of Refs. [32–34], does not necessarily produce the most deterministic looking $W(\Delta)$. Since $W=1$ is supposed to hold for any $\{c_r\}$, the choice of vector field is arbitrary. We choose ten vector fields, first chosen by Salvino and Cawley [35], and identify maximum and minimum values of the $W(\Delta)$ for each time delay Δ.

The method, which estimates the average of the directional elements after partitioning the phase space by uniform grids, may present spurious results for inhomogeneous vector fields in the phase space. The value of the mean directional elements in a box depends on the number of data points in a box. If we partition the phase space by a coarse-grained uniform grid, the dense regions would have excessively large points in one box, which then leads to low values of W even for smooth data. On the other hand, if there are only one or a few points in the boxes with finely grained meshes, they would give rise to relatively high values for W. It is very difficult to partition the phase space by a proper size of grids in a high-dimensional phase space, because the number of boxes is exponentially increasing as the size of the boxes decreases. Unfortunately, most of the dynamical systems in nature are both high-dimensional and inhomogeneous.

We modified the method in order to overcome these problems. First, we picked a random point in the phase space, and then we chose the nearest-neighbor points around this random center. We selected $d+1$ for the number of the nearest neighbors around this random center, where d is the embedding dimension. Then we estimated the mean directional elements in that box, and iterated it.

In the test, we introduced an informal determinism tolerance criterion: if $0.9<W<1.0$, then we would label the given data as deterministic, and if $0<W<0.7$, then we would conclude there is no evidence for determinism. The intermediate case, $0.7<W<0.9$, is known to sometimes arise from a deterministic time series [36]. In these cases we would necessarily compare the results with those for the surrogate data.

Figure 1 shows the comparison of the W plots for the data of Rössler systems obtained from (a) our method with those from (b) the Salvino-Cawley method. For the Rössler time series the x coordinate of $\dot{x}=-(y+z),\dot{y}=x+0.15y,\dot{z}=0.2$

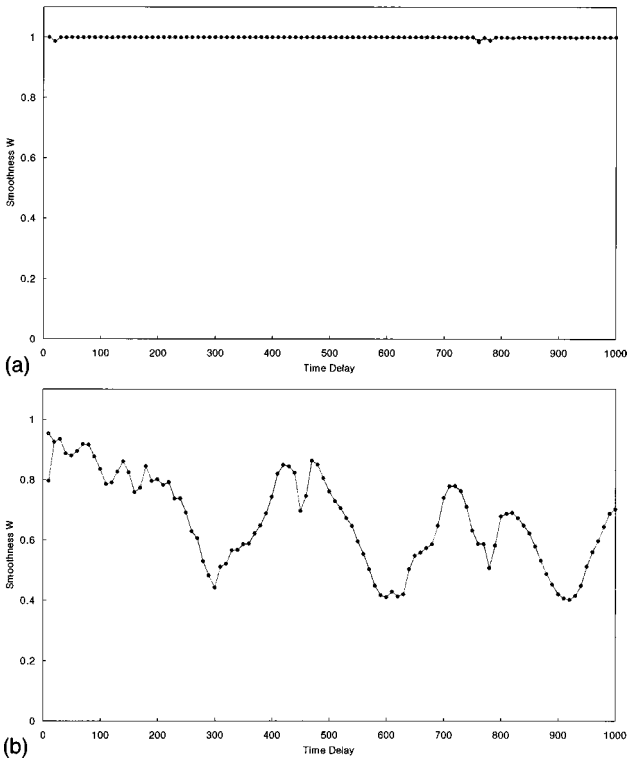

FIG. 1. The comparison of W plots obtained from our method with the original one: For each time delay $\triangle$, computed W values are maximum ($\bullet$) and minimum ($\diamond$) for Rössler system (a) with our method; (b) with the original method.

$+zx-10z$ was sampled with $\Delta t=0.004$. The number of data points is 20 000 and the embedding dimension is 5. While the number of boxes in the original algorithm is $40\times40\times40\times40\times40$, the number of random centers is 2000 in our method. Computed W values shown are maxima ($\bigcirc$) and minima ($\diamond$) for each different time delay Δ over ten arbitrarily chosen vector fields. However, there are little differences between maxima and minima. With our method the maximum and minimum values of W are nearly 1 over all time delays, and are more stable than those with the Salvino-Cawley method. We can find from Fig. 1(b) that the W values obtained from the original method are periodically decreased at the time delays of the multiples of 300, which may be caused by the dynamical structure of the Rössler attractor in the phase space.

Figure 2 depicts the W plots for the data from (a) the Lorenz system and (b) the Henon map. We computed W values for the Lorenz system $[\dot{x}=10(y-x),\dot{y}=28x-y-xz,\dot{z}=-\frac{8}{3}z+xy]$, with sampling time $\Delta t=0.004$, and the Henon map $[x_i=y_{i-1}+1-1.4x_{i-1}^2,y_i=0.3x_{i-1}]$ data. The W values for the Lorenz equation and the Henon map are stable around 0.94 for each time delay. This means by an informal determinism tolerance criterion that they are generated from deterministic systems. Maximum W values for both of them were also about 0.91 in the original method [35].

We used the minimum embedding dimension in an embedding procedure for reconstructing the attractors in the phase space. We estimated the minimum embedding dimension using the method presented by Kennel *et al.* [42]. The

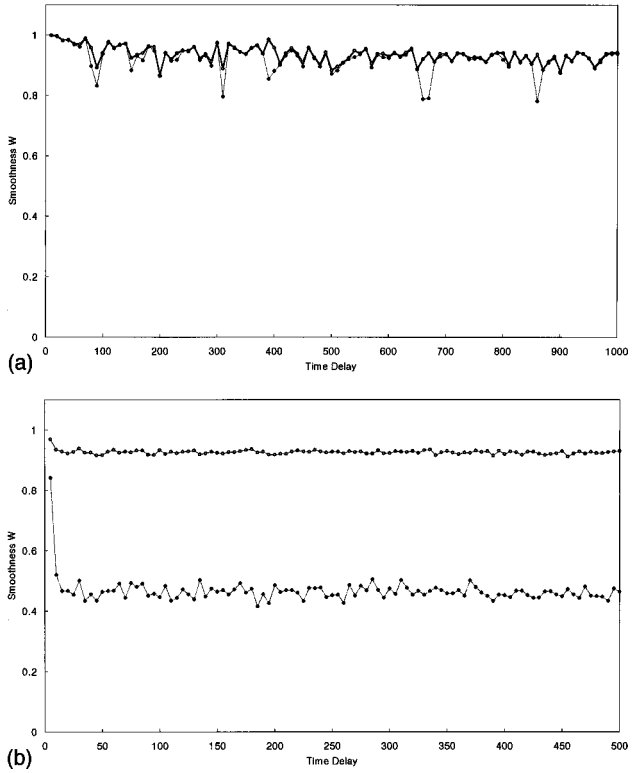

FIG. 2. $W(\triangle)$ plots for the data from (a) Lorenz system and (b) Henon map. W values shown are maximum ($\bullet$) and minimum ($\diamond$) for each $\triangle$.

basic idea of the method is that in the passage from dimension d to dimension $d+1$, one can differentiate points on an orbit which are true neighbors from those on the orbit which are false neighbors. A false neighbor is a point in the data set that is a neighbor solely because we are viewing the orbit (the attractor) in too small an embedded space ($d<d_{\min}$). When we have achieved a large enough embedding space ($d\geqslant d_{\min}$), all neighbors of every orbit point in the multivariate phase space will be true neighbors. A detailed procedure is presented in Ref. [42].

We define the embedding rate as the ratio of the true neighbors to the neighbors in the embedding dimension. Figure 3 displays a typical example of the embedding rate as a function of the embedding dimension for 16 384 EEG data points at T_4 in a subject. The proper minimum embedding dimension was selected as 11 in this case.

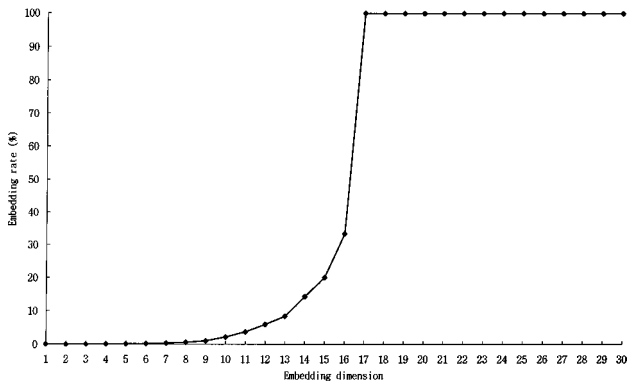

FIG. 3. The embedding rate as a function of embedding dimension for 16 384 EEG data points of a subject.

III. TEST FOR DETERMINISM IN EEG

There are four main steps to our test. First, we recorded the EEG data from normal subjects. Second, we reduced the additive noise in the EEG with a nonlinear method, developed by Sauer. Third, we measured the smoothness of the EEG. Fourth, we compared the results from the EEG with those from the surrogate data.

The EEG data were recorded from five subjects (two men and three women; age $= 22.1 \pm 3.8$ years, mean$\pm$S.D.), who are healthy individuals with no history of psychiatric or neurological disease, at St. Mary's Hospital in Taejon. With the subjects in a relaxed state with closed eyes, 32.768 sec of data (16 384 data points with sampling time $\Delta t = 2$ ms) were recorded with a Nihon Kohden EEG-4421K, and then digitized by a 12-bit analog-digital converter in an IBM PC. Recordings were made under the eyes-closed condition in order to obtain as long of a stationary EEG data as possible. All data were digitally filtered in order to remove the residual EMG activity at 1–35 Hz.

An important experimental fact in chaotic data analysis is the ubiquitous presence of noise in the time series. Noise, whether measurement noise, which is merely additive, or dynamical noise, whose origin lies in the dynamical process itself, can obscure the smoothness feature of a phase portrait. Thus it is important to incorporate noise reduction in order to make a smoothness test for determinism robust. It is problematic to apply linear filtering techniques for noise reduction to nonlinear systems, since the power spectrum of the chaotic deterministic signal as well as the noise may be broadband. Recently several nonlinear noise-reduction methods were proposed in application to nonlinear dynamical signals [43–49]. Successful application of a nonlinear noise reduction algorithm can recover phase-space smoothness, which was lost under the influence of noise.

We used the nonlinear method that is developed by Sauer [48]. This method used a filtered version of delay coordinate embedding called a low-pass embedding, and the singular value decomposition in projecting the input signal along directions belonging to the signal of interest. The method is iterative in nature. One pass of the algorithm through the data replaces an original time series $\{s_i : 1 \leqslant i \leqslant L\}$ by a less noisy version of the original series $\{s_i' : 1 \leqslant i \leqslant L\}$. Then the same process can be applied to the new series, and so forth. The new time series is determined by $s_i' = s_i + m(\hat{t}_i - s_i)$, where $\hat{t}_i$ is the average value of the several correct values t_{ij} of s_i, and where $0 \leqslant m \leqslant 1$ is a factor fixed for the entire pass through the data. We typically use $m = 0.1$ for the first pass, and then slowly increase m to 0.5 throughout further passes.

There are four steps to generate the estimates t_{ij} of the correct value of s_i: low-pass embedding, neighborhood selection, singular value decomposition, and a correction decorrelation step. First, the data are embedded using coordinates that are smoothed locally in time using the Fourier transform (low-pass embedding). For a chosen window size of length w, the discrete Fourier transform on w points is evaluated. The Fourier components corresponding to the $\frac{1}{2}d$ lowest frequencies are kept for some even integer $d < w$, where d is an embedding dimension. The value of w was 64 and d was 16 in this case. The inverse transform on d points yields a smoothed version of a windowed section of the signal. The second step is to organize the embedded points in neighborhoods of size r, where r is a rough estimate of the size of the noise. The third step is to project the points in the neighborhood onto the attractor, or at least to push the points in that direction using the singular value decomposition to calculate the principal directions of the set of vectors which connect fixed base points to the embedded points. After the corrections necessary to project the points onto the principal directions are determined, we then make use of the fact that the noise is uncorrelated with the signal of interest. For each embedding coordinate, the random noise in that coordinate has an expected value of zero. In order to minimize the introduction of new correlations in the noise from our algorithm, a postprocessing of the corrections to ensure that they add to zero also is needed (correction decorrelation step). The algorithm is described in more detail in the paper by Sauer [48].

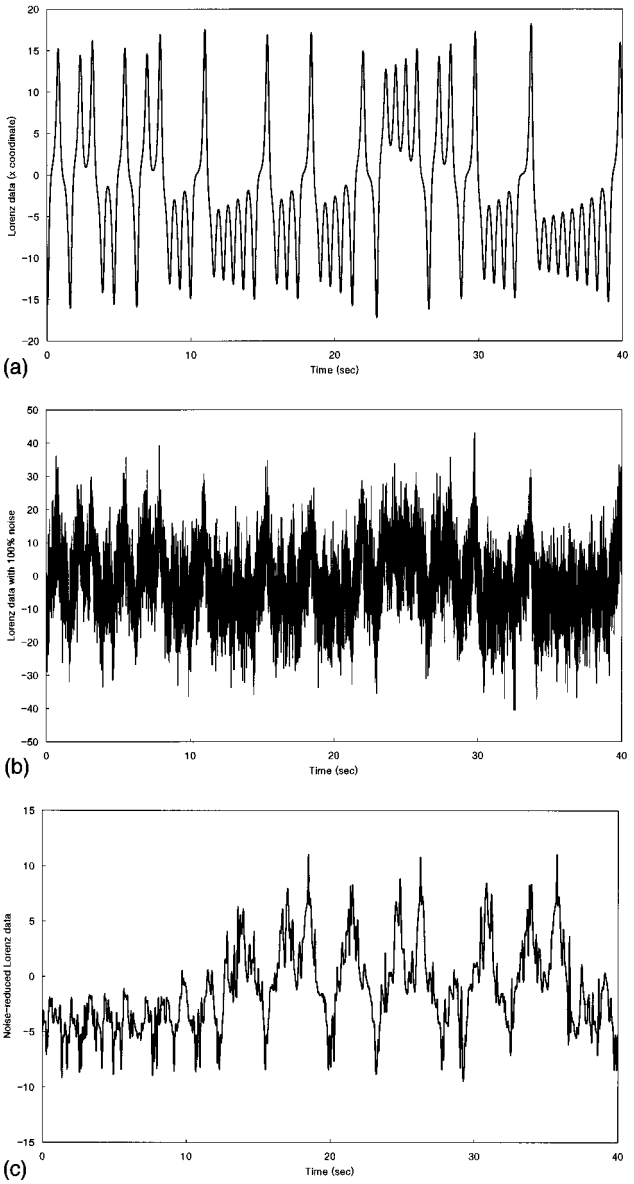

FIG. 4. (a) Lorenz x coordinate times series, (b) Lorenz data corrupted by 100% white Gaussian noise (0 dB), (c) noise-reduced Lorenz data by the nonlinear method developed by Sauer.

Figure 4 illustrates the effect of the noise-reduction

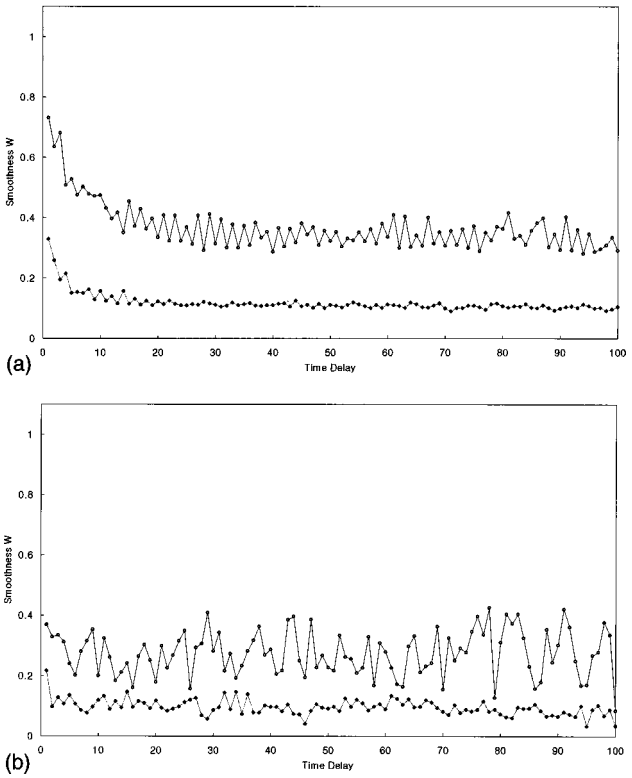

FIG. 5. *W* plots for (a) the raw data and (b) the surrogate data of an EEG from a subject before application of the noise-reduction method. For each $\triangle$, *W* values shown are maximum ($\bullet$) and minimum ($\diamond$).

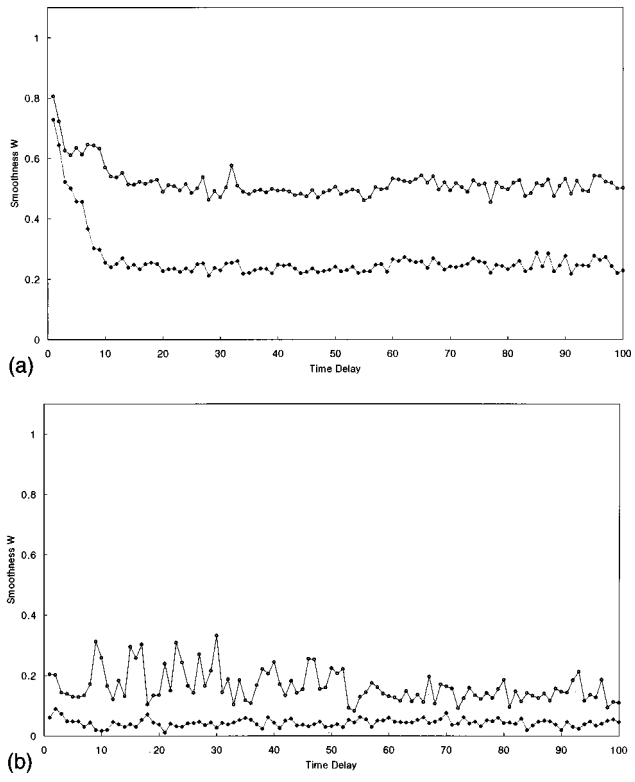

FIG. 6. *W* plots for (a) the raw data and (b) the surrogate data of the EEG from a subject after application of the noise-reduction method.

method on the noise mixed with the signal. It shows (a) noise-free Lorenz data, (b) Lorenz data with 100% white Gaussian noise (0 dB), and (c) noise-reduced Lorenz data with our method. A nonlinear noise reduction algorithm can recover smoothness of the Lorenz data lost under the influence of noise. However, as shown in the study of Cawley *et al.*, nonlinear noise reduction does not create smooth phase portraits [36].

A simple comparison test using a surrogate time series can distinguish smoothness from nonsmooth behavior for chosen types of randomness. The algorithm of generating surrogate data is based on the null hypothesis, which states that the data come from a linear Gaussian process [50]. The surrogate data are constructed to have the same Fourier spectra as the raw data. The Fourier transform has a complex amplitude at each frequency, to randomize the phases. We multiply each complex amplitude by $\exp[i\phi]$, where ϕ is independently chosen for each frequency from the interval $[0,2\pi]$.

Figure 5 shows the *W* plots for (a) the raw and (b) the surrogate data of the EEG at channel T_4 from a subject before noise reduction. The embedding dimension *d* is 16 and, consequently, the number of neighbors around a random center is 17 (Fig. 5). The number of data points is 16 384. The number of random centers is 1500. For each Δ, the maximum ($\bigcirc$) and minimum ($\diamond$) values of *W* are shown in the figure. The maximum and minimum values of *W* for the raw EEG data in Fig. 5(a) are oscillating around 0.38 and 0.13, respectively, which implies that the EEG is not a deterministic signal. The results for the surrogate EEG data are slightly below those for the raw EEG, i.e., 0.36 for average maximum *W* and 0.09 for average minimum W in Fig. 5(b). *W* values for the surrogate EEG are more fluctuating than those for the raw EEG. There are little differences in the *W* plots for the EEGs from different channels in a subject. The EEGs of ten subjects also have similar values for *W*. The average values of stable maxima and minima *W* for the raw EEGs of ten subjects with standard deviations are 0.4 ± 0.08 and 0.14 ± 0.04, respectively.

After application of the noise reduction method, the average values of maximum *W* for the EEG increased up to 0.52, however they do not exceed 0.7,a minimum deterministic tolerance for determinism as shown in Fig. 6(a). The maximum values of *W* for the surrogate EEG are staying under 0.2 [Fig. 6(b)]. We can detect from Fig. 6 that the noise-reduced version of the raw EEG has highly different values for *W* from the surrogate data of the EEG, even though the *W*'s of the noise-reduced raw EEG are under 0.7. We can infer from this result that the EEG can be somewhat distinguished from the surrogate signal generated by a linear stochastic process.

IV. TEST FOR HIGH-DIMENSIONAL DETERMINISM

As a result, our test suggests that the EEG does not have any determinism. However, we can also include some possibilities for determinism in an EEG. One of the possibilities is that the determinism in the EEG is too high-dimensional to be detected with current methods including our method. The present method may detect only low-dimensional determinism in a time series. The EEG, however, can be assumed to

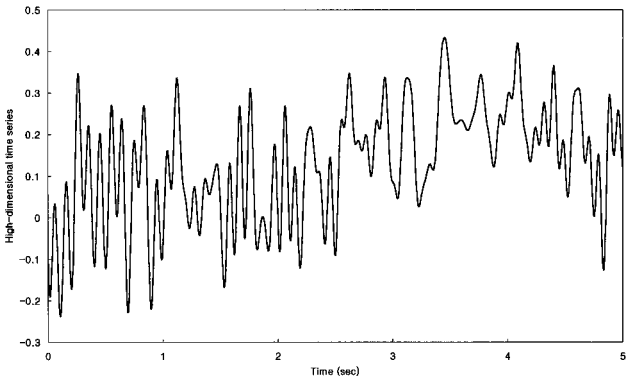

FIG. 7. A time series generated from a high-dimensional system in this study.

be generated from high-dimensional systems.

We examined the applicability of our method to high-dimensional signals by generating an EEG-like signal from high-dimensional differential equations. We generated the high-dimensional signal from nonlinear equations of 12 variables including the Lorenz equation, the Ueda equation, the two-well potential Duffing-Holmes equation, and the Rössler equation. The degrees of freedom of the EEG can be assumed to be about 12 since the correlation dimensions of the normal EEGs were reported between 6 and 13 [15,51]. The EEG-like signal generated from these equations also had a power spectrum in the range of 0.2–12 Hz, similar to dominant frequency ranges of EEGs.

The nonlinear coupled equations are

$$\dot{x}_1 = x_2, \tag{5}$$

$$\dot{x}_2 = \frac{(x_5 - 25)}{3}\sin \omega_1 t + 3x_7 \sin \omega_2 t + x_{11} \sin \omega_3 t - 3|x_6|x_2 - x_9 x_1, \tag{6}$$

where $\omega_1 = 30.0, \omega_2 = 65.0, \omega_3 = 80.0$. They are coupled with other equations as follows:

$$\dot{x}_3 = \sigma(x_4 - x_3), \tag{7}$$

$$\dot{x}_4 = -x_3 x_5 + r x_3 - x_4, \tag{8}$$

$$\dot{x}_5 = x_3 x_4 - b x_5, \tag{9}$$

where $\sigma = 10.0, r = 28.0, b = 8/3$ (Lorenz equation);

$$\dot{x}_6 = x_7, \tag{10}$$

$$\dot{x}_7 = -k x_7 - x_6^3 + B \cos t, \tag{11}$$

where $k = 0.1, B = 12.0$ (Ueda equation);

$$\dot{x}_8 = x_9, \tag{12}$$

$$\dot{x}_9 = -\delta x_9 + \frac{1}{2} x_8 (1 - x_8^2) + f \cos \omega t, \tag{13}$$

where $\delta = 0.15, F = 0.15, \omega = 0.8$ (two-well potential Duffing-Holmes attractor);

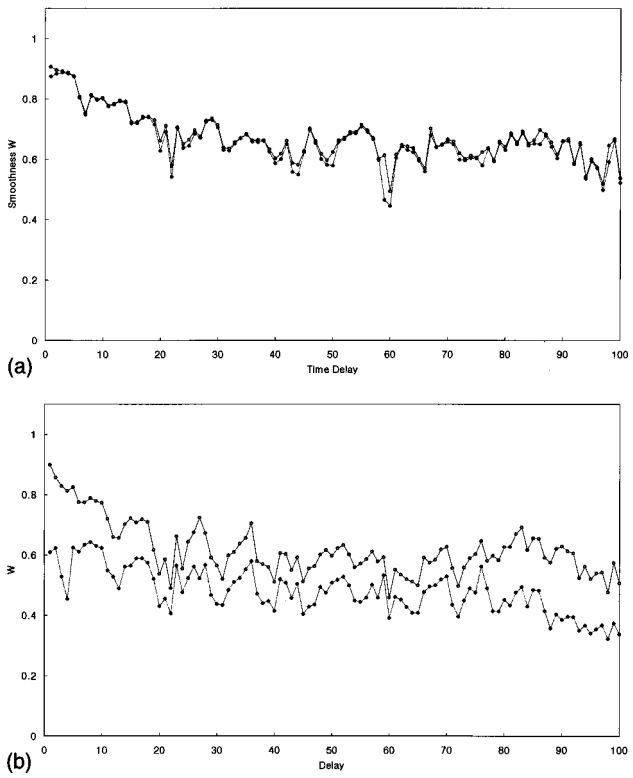

FIG. 8. W plots for (a) a time series generated from a high-dimensional deterministic system and for (b) surrogated data of the time series. For each $\triangle$, W values shown are maximum ($\bullet$) and minimum ($\diamond$).

$$\dot{x}_{10} = -(x_{11} + x_{12}), \tag{14}$$

$$\dot{x}_{11} = x_{10} + \alpha x_{11}, \tag{15}$$

$$\dot{x}_{12} = \alpha + x_{12}(x_{10} - \mu), \tag{16}$$

where $\alpha = 0.15, \mu = 10.0$ (Rössler attractor).

We used the x_1 coordinate solution $x_1(t)$ for the signal shown in Fig. 7. It is very similar to the EEG with a visual inspection. Figure 8 demonstrates the W plots for (a) the signal and (b) the surrogate data of the signal. 18 is used for the embedding dimension and 1500 random centers are used in our method. The maximum and minimum values of W decrease over time delays to below 0.7, and then stably oscillate around 0.6. It indicates that this method cannot detect high-dimensional determinism from the time series.

As is well known, many real systems may be high-dimensional. If they have too many degrees of freedom, it may be necessary to regard them as effectively random for all practical purposes. Indeed, the effort to use the data analysis methods developed for nonlinear dynamics only makes sense when the system is low-dimensional [37]. Thus current methods, including ours, need to be improved to be applicable for the time series generated from high-dimensional systems, even though some recent studies propose new methods applicable to high-dimensional systems [38].

V. CONCLUSION

We tested determinism in an EEG by detecting smoothness of vector fields reconstructed from a time series of the EEG. We were not able to find any evidence for determinism in the EEG from the test. However, we cannot exclude the possibility that EEGs are of too high a dimension for their determinism to be detected with current methods. It is very important to develop direct methods applicable to the experimental time series from high-dimensional systems, such as biological systems. Furthermore, these methods need to be applied to a time series from many kinds of experimental systems.

ACKNOWLEDGMENTS

We thank Dr. Dae-jin Kim and J. Lee at St. Mary's Hospital in Taejon for experimental help during this study.

[1] A. Babloyantz, J. M. Salazar, and C. Nicolis, Phys. Lett. **111A**, 152 (1985).
[2] A. Babloyantz, in *Dynamics of Sensory and Cognitive Processing by the Brain*, edited by E. Başar (Springer, Berlin, 1988), p. 196.
[3] J. Röschke and E. Başar, in *Dynamics of Sensory and Cognitive Processing by the Brain* (Ref. [2]), p. 203.
[4] A. C. K. Soong and C. I. J. M. Stuart, Biol. Cybern. **62**, 55 (1989).
[5] R. Friedrich, A. Fuchs, and H. Haken, in *Rhythms in Biological System*, edited by H. Haken and H. P. Köpchen (Springer, Berlin, 1992), p. 315.
[6] H. Haken, *Principles of Brain Functioning* (Springer-Verlag, Berlin, 1996), p. 193.
[7] R. Friedrich and C. Uhl, Physica D **98**, 171 (1996).
[8] A. Babloyantz and A. Destexhe, in *From Chemical to Biological Organization*, edited by M. Markus, S. Muller, and G. Nicolis (Springer, Berlin, 1987), p. 307.
[9] J. P. Pijn, J. Van Neerven, A. Noest, and F. H. Lopes da Silva, Electroencephalogr. Clin. Neurophysiol. **79**, 371 (1991).
[10] J. Röschke and J. Aldenhoff, Biol. Cybern. **64**, 307 (1991).
[11] J. Wackermann, D. Lehmann, I. Dvorak, and C. M. Michel, Electroencephalogr. Clin. Neurophysiol. **86**, 193 (1993).
[12] G. W. Frank, T. Lookman, M. A. H. Nerenberg, and C. Essex, Physica D **46**, 427 (1990).
[13] J. Fell, J. Röschke, and P. Beckmann, Psychiat. Res. **56**, 257 (1995).
[14] C. J. Stam, B. Jelles, H. A. M. Achtereekte, J. H. van Birgelen, and J. P. J. Slaets, Clin. Electroenceph. **27**, 69 (1996).
[15] J. Jeong, S. Y. Kim, and S. H. Han, Electroencephalogr. Clin. Neurophysiol. **106**, 220 (1998).
[16] K. Lehnertz and C. Elger, Phys. Rev. Lett. **80**, 5019 (1998).
[17] K. Kopitzki, P. C. Warnke, and J. Timmer, Phys. Rev. E **58**, 4859 (1998).
[18] J. Theiler, Phys. Rev. A **34**, 2427 (1986).
[19] L. Glass and M. C. Mackey, *From Clocks to Chaos: The Rhythms of Life* (Princeton University Press, Princeton, 1988).
[20] P. Grassberger, T. Schreiber, and C. Schaffrath, Int. J. Bifurcation Chaos Appl. Sci. Eng. **1**, 521 (1991).
[21] J. P. Eckmann and D. Ruelle, Physica D **56**, 185 (1992).
[22] A. R. Osborne and A. Provenzale, Physica D **35**, 357 (1989).
[23] P. E. Rapp, A. M. Albino, T. I. Schmah, and L. A. Farwell, Phys. Rev. E **47**, 2289 (1993).
[24] J. Theiler, S. Eubank, A. Longtin, B. Galdrikian, and J. D. Farmer, Physica D **58**, 77 (1992).
[25] J. Theiler and P. Rapp, Electroencephalogr. Clin. Neurophysiol. **98**, 213 (1996).
[26] W. S. Pritchard, D. W. Duke, and K. K. Krieble, Psychophysiology **32**, 486 (1995).
[27] M. Casdagli, J. R. Stat. Soc. B **54**, 303 (1992).
[28] S. A. R. B. Rombouts, R. W. M. Keunen, and C. J. Stam, Phys. Lett. A **202**, 352 (1995).
[29] M. Palus, Biol. Cybern. **75**, 389 (1996).
[30] G. Sugihara and R. M. May, Nature (London) **344**, 734 (1990).
[31] M. B. Kennel and S. Isabelle, Phys. Rev. A **46**, 3111 (1992).
[32] D. T. Kaplan and L. Glass, Phys. Rev. Lett. **68**, 427 (1992).
[33] D. T. Kaplan and L. Glass, Physica D **64**, 431 (1993).
[34] R. Wayland, D. Broomley, D. Pickett, and A. Passamante, Phys. Rev. Lett. **70**, 580 (1993).
[35] L. W. Salvino and R. Cawley, Phys. Rev. Lett. **73**, 1091 (1994).
[36] R. Cawley, G.-H. Hsu, and L. W. Salvino, in *Chaotic, Fractal, and Nonlinear Signal Processing*, edited by R. A. Katz (AIP Press, New York, 1996), p. 55.
[37] R. Cawley, G.-H. Hsu, and L. W. Salvino, in *Predictability of Complex Dynamical System*, edited by Y. A. Kravtsov and J. B. Kadtke (Springer-Verlag, Berlin, 1996), p. 23.
[38] G. J. Ortega and E. Louis, Phys. Rev. Lett. **81**, 4345 (1998).
[39] K. J. Blinowska and M. Malinowski, Biol. Cybern. **66**, 159 (1991).
[40] A. I. Mees, in *Nonlinear Modeling and Forecasting*, edited by M. Casdagli and S. Eubank, Proceedings of the Workshop on Nonlinear Modeling and Forecasting (Addison-Wesley Publishing Company, New York, 1992), p. 3.
[41] L. Glass, D. T. Kaplan, and J. E. Lewis, in *Proceedings of the Second Annual Conference on Nonlinear Dynamical Analysis of the EEG*, edited by B. H. Jansen and M. E. Brandt (World Scientific, Singapore, 1993), p. 233.
[42] M. B. Kennel, R. Brown, and H. D. I. Abarbanel, Phys. Rev. A **45**, 3403 (1992).
[43] E. Kostelich and J. Yorke, Phys. Rev. A **38**, 1649 (1988).
[44] E. Kostelich and J. Yorke, Physica D **41**, 183 (1990).
[45] S. Hammel, Phys. Lett. A **149**, 421 (1990).
[46] T. Schreiber and P. Grassberger, Phys. Lett. A **160**, 411 (1991).
[47] J. D. Farmer and J. Sidorowich, Physica D **47**, 373 (1991).
[48] T. Sauer, Physica D **58**, 193 (1992).
[49] R. Cawley and G. H. Hsu, Phys. Rev. A **46**, 3057 (1992).
[50] J. Theiler, S. Eubank, A. Longtin, B. Galdrikian, and J. D. Farmer, Physica D **58**, 77 (1992).
[51] C. Besthorn, H. Sattel, C. Geiger-Kabisch, R. Zerfass, and H. Forstl, Electroencephalogr. Clin. Neurophysiol. **95**, 84 (1995).